Published in final edited form as:
Dev Cell. 2012 July 17; 23(1): 97–111. doi:10.1016/j.devcel.2012.05.011.

Two Forkhead transcription factors regulate the division of cardiac progenitor cells by a Polo-dependent pathway

Shaad M. Ahmad[1], **Terese R. Tansey**[1], **Brian W. Busser**[1], **Michael T. Nolte**[2], **Neal Jeffries**[3], **Stephen S. Gisselbrecht**[4], **Nasser M. Rusan**[5], and **Alan M. Michelson**[1,*]

[1]Laboratory of Developmental Systems Biology, Genetics and Developmental Biology Center, National Heart Lung and Blood Institute, National Institutes of Health, Bethesda, MD 20892, United States

[2]Department of Biological Sciences, University of Notre Dame, Notre Dame, IN 46556, United States

[3]Office of Biostatistics Research, National Heart Lung and Blood Institute, National Institutes of Health, Bethesda, MD 20892, United States

[4]Division of Genetics, Department of Medicine, Brigham and Women's Hospital and Harvard Medical School, Boston, MA 02115, United States

[5]Laboratory of Molecular Machines and Tissue Architecture, Cell Biology and Physiology Center, National Heart Lung and Blood Institute, National Institutes of Health, Bethesda, MD 20892, United States

SUMMARY

The development of a complex organ requires the specification of appropriate numbers of each of its constituent cell types, as well as their proper differentiation and correct positioning relative to each other. During *Drosophila* cardiogenesis, all three of these processes are controlled by *jumeau* (*jumu*) and *Checkpoint suppressor homologue* (*CHES-1-like*), two genes encoding forkhead transcription factors that we discovered utilizing an integrated genetic, genomic and computational strategy for identifying genes expressed in the developing *Drosophila* heart. Both *jumu* and *CHES-1-like* are required during asymmetric cell division for the derivation of two distinct cardiac cell types from their mutual precursor, and in symmetric cell divisions that produce yet a third type of heart cell. *jumu* and *CHES-1-like* control the division of cardiac progenitors by regulating the activity of Polo, a kinase involved in multiple steps of mitosis. This pathway demonstrates how transcription factors integrate diverse developmental processes during organogenesis.

INTRODUCTION

The remarkable cellular diversity present within metazoan organs illustrates several important themes in developmental biology, including a requirement for the specification of appropriate numbers of distinct cell types, the proper differentiation of these cells and their

*Author for correspondence: michelsonam@mail.nih.gov, Phone: 301-451-8041, Fax: 301-496-9985.

Accession numbers
Microarray data utilized in this study are available from the Gene Expression Omnibus (www.ncbi.nlm.nih.gov/geo) with the accession numbers GSE3854, GSE29573 and GSE34946.

correct positioning within the organ (Rosenthal and Harvey, 2010). Taken together, the existence of multiple organ-specific cell types implies that numerous biological processes must work in unison during development, and raises an intriguing question: how is the requisite integration of these diverse developmental pathways achieved?

The formation of the *Drosophila* embryonic heart provides a particularly amenable system for addressing this question (Bodmer and Frasch, 2010; Bryantsev and Cripps, 2009). An organ that pumps hemolymph throughout the body cavity, the *Drosophila* heart is composed of two groups of cells arranged in a metamerically repeated and stereotyped pattern (Figures 1A-1C): an inner group of *Myocyte enhancer factor 2* (*Mef2*)-expressing contractile cardial cells (CCs) that form a linear tube, surrounded by a sheath of *pericardin* (*prc*) and *Zn finger homeodomain 1* (*zfh1*)-expressing nephrocytic pericardial cells (PCs). Neither the CCs nor the PCs constitute a uniform population, as revealed both by their distinct cell lineages and by the complexity of their individual gene expression programs. From anterior to posterior, and named for the transcription factors they express, there are two Seven-up-CCs (Svp-CCs), two Tinman-Ladybird-CCs (Tin-Lb-CCs), and two CCs expressing only Tin (the posterior-most Tin-CCs) in each hemisegment. A larger number of PCs surround the cardial cells: 2 Svp-PCs and 2 Odd-skipped-PCs (Odd-PCs) are positioned laterally, 2 Even-skipped-PCs (Eve-PCs) are situated dorsolaterally, and a row of Tin-PCs and Tin-Lb-PCs runs immediately ventral to the CCs (Azpiazu and Frasch, 1993; Bodmer, 1993; Jagla et al., 1997; Ward and Skeath, 2000).

A stereotyped series of asymmetric and symmetric cardiac progenitor cell divisions gives rise to these eight differentiated cell types (Alvarez et al., 2003; Han and Bodmer, 2003). The differential expression of multiple genes, and both the distinct lineage and intricate but invariant positioning of the individual heart cell types, argue for a high degree of functional precision and regulatory complexity in the generation of the heart. This hypothesis is borne out by classical genetic studies, which showed that the development of the *Drosophila* heart from the dorsal-most region of the mesoderm, a *tin*-expressing domain referred to as the cardiac mesoderm (CM), is dependent on contributions from multiple signals and transcription factors that are conserved between flies and vertebrates (summarized in Figure 1D; reviewed by Bodmer and Frasch, 2010; Bryantsev and Cripps, 2009; Chien et al., 2008). Thus, the identification of genes that regulate cardiac development, and detailed investigations of their expression and function in *Drosophila*, are likely to provide considerable insight into the related mechanisms controlling cardiogenesis in vertebrates, including human.

Here, we describe an integrated strategy that we developed and applied to identify 70 genes expressed in the *Drosophila* CM or heart. We further show that one gene discovered with this approach, *jumeau* (*jumu*), plus its homolog, *Checkpoint suppressor homologue* (*CHES-1-like*)—both of which encode Fkh transcription factors—mediate both asymmetric and symmetric cardiac progenitor cell divisions by regulating a Polo-kinase dependent pathway.

RESULTS

A genomic screen for genes expressed in the cardiac mesoderm or heart

As an initial step to identify regulators and effectors of heart development in *Drosophila*, we screened for genes expressed in the CM or differentiated heart using an integratedgenetic, genomic and computational strategy that we previously applied to study somatic muscle gene expression (Estrada et al., 2006). Two essential aspects of our approach are the use of specific genetic backgrounds to selectively perturb CM gene expression based on prior knowledge of cardiogenic pathways (Figures 1D-1E), and the availability of a training set of

40 genes already known to be expressed in the CM. Previous studies revealed that activation of the fibroblast growth factor receptor (FGFR)- and epidermal growth factor receptor (EGFR)-driven receptor tyrosine kinase (RTK)/Ras, Wingless (Wg) or Decapentaplegic (Dpp) pathways produces extra CM cells compared with wild-type, thereby elevating levels of CM gene expression (Azpiazu and Frasch, 1993; Bodmer, 1993; Carmena et al., 1998; Frasch, 1995; Gisselbrecht et al., 1996; Grigorian et al., 2011; Michelson et al., 1998; Staehling-Hampton et al., 1994). In contrast, activation of Notch results in fewer CM cells and thus reduced levels of CM gene expression (Hartenstein et al., 1992; Mandal et al., 2004). Moreover, since the CM arises from the *tin*-expressing dorsal mesoderm, CM genes will be highly enriched in cells purified from this subregion of the whole embryo.

To generate a compendium of gene expression profiles associated with CM development, we used flow cytometry to purify the entire mesoderm from both wild-type stage 11 embryos and similar embryos from 9 informative genetic backgrounds, as well as *tin*-expressing dorsal mesoderm from equivalently staged wild-type embryos (Figure 1E). We then used a statistical meta-analysis method (Estrada et al., 2006) fitted to the training set of 40 known CM genes to rank all *Drosophila* genes by their likelihood of being expressed in the CM based on their collective behavior in this expression profiling compendium. Any gene that (i) is upregulated with activation of the RTK/Ras, Wg or Dpp pathways, upregulated with *Dl* loss-of-function, downregulated with Notch activation, and downregulated with *wg* loss-of-function, and (ii) is enriched in *tin*-expressing mesoderm relative to the entire mesoderm, has a high probability of being expressed in the CM (Table S1A, Experimental Procedures).

To validate the predictions of this meta-analysis, we used large-scale whole-embryo in situ hybridizations to assess the in vivo expression patterns of highly ranked CM gene candidates. Of 136 randomly selected genes that provided informative in situ hybridization results among the top-ranked 400 candidates, and which did not include any of the training set genes, 70 were expressed in the CM and/or heart. Thus, the meta-analysis predicted cardiac genes with an accuracy of 51.4% (Table S1B). Further analyses revealed that 37 genes are expressed in both the CM and the mature heart, 22 genes are expressed in the CM but not in the heart, and 11 genes are expressed in the heart but not in the CM (Table S1B and Figure S1).

To gain insight into the biological processes in which these genes are involved, the 110 training set plus newly validated CM and heart genes were queried for the relative enrichment of Gene Ontology (GO) terms. Overrepresented terms (Table S1C) include categories associated with mesoderm development, cardiac differentiation, cell fate specification, transcriptional regulation, migration, tube morphogenesis and the RTK/Ras pathway. Another enriched category was nervous system development, which likely reflects the pleiotropic effects of many developmental regulators, and the fact that many of the identified genes are also expressed in the nervous system (data not shown). Among the unexpected overrepresented categories were cytokinesis and cell division, the relevance of which became apparent upon a detailed analysis of the cardiogenic functions of *jumu, CHES-1-like* and *polo*.

The Fkh genes *jumu* and *CHES-1-like* are involved in *Drosophila* heart development

Previous studies have shown a striking conservation of transcription factors involved in both *Drosophila* and vertebrate cardiogenesis. Genes encoding transcription factors were also overrepresented among the 110 CM- and heart-expressed genes. One such gene is *jumu*, which encodes a Fkh subclass N transcription factor (Lee and Frasch, 2004) that is continuously expressed in the CM and differentiating heart from embryonic stages 11 to 13 (Figures 2A and S1Y-S1Y’’’). In addition, we examined the expression pattern of the only

other *Drosophila* Fkh subclass N gene, *CHES-1-like*, and found that it is also expressed in the CM during stages 11 and 12 (Figures 2B and S1Z-S1Z’’’).

Given the presence of these two Fkh transcription factors in the embryonic CM, and the fact that this class of proteins is involved in mammalian cardiogenesis, we next used a whole embryo RNA interference (RNAi) assay to assess whether *jumu* and *CHES-1-like* play a role in *Drosophila* cardiac development. RNAi directed against either *jumu* or *CHES-1-like* resulted in incorrect numbers and an uneven distribution of both CCs and PCs (Figures 2C-2E), indicating that both of these Fkh factors are essential for normal heart development.

Loss of either jumu or CHES-1-like function results in localized changes in cardial cell number, giant nuclei and incorrectly positioned heart cells

We undertook a more detailed analysis of the cardiogenic effects of *jumu* and *CHES-1-like* by examining the phenotypes associated with loss-of-function mutations in these genes. Staining with antibodies against the nuclear protein Mef2 (which is expressed in CCs of the heart, as well as in somatic myoblasts) revealed that the uniform and symmetrically aligned distribution of CCs seen in wild-type embryos (Figure 2F) is markedly disrupted in embryos homozygous for *jumu* hypomorphic mutations ($jumu^{06439}$ and $jumu^{Df2.12}$, Figure 2G-2H), a *jumu* null deficiency (*Df(3R)Exel6157*, Figure 2I) which deletes both *jumu* and another gene not involved in heart development (Cheah et al., 2000; Strodicke et al., 2000; see also Table S2), and a null mutation that we generated in *CHES-1-like* ($Df(1)CHES\text{-}1\text{-}like^{1}$, Figures 2J and S2; see Experimental Procedures).

Each mutant exhibited different hemisegments having localized increases or decreases in CC number, occasional enlarged CC nuclei, or CCs which were misaligned with other CCs within a hemisegment or with their counterparts across the dorsal midline. Similar phenotypes were also observed when either *jumu* or *CHES-1-like* activity was knocked down by CM-targeted RNAi directed by the *Hand-GAL4* and *tinD-GAL4* drivers (Figure 2K-2L), indicating that the requirement of these Fkh genes for correct heart development is autonomous to the cardiac mesoderm. Embryos doubly homozygous for both the *jumu* null deficiency and the *CHES-1-like* null mutation exhibited a more severe phenotype, often missing entire hemisegments of CCs (Figure 2M). Taken together, these results suggest a role for abnormal cell division as the origin of the *jumu* and *CHES-1-like* mutant heart phenotypes, which is consistent with the known involvement of *jumu* in nervous system development (Cheah et al., 2000).

jumu and *CHES-1-like* are required for both asymmetric and symmetric divisions of cardiac progenitor cells

Two asymmetric progenitor cell divisions generate all the Svp-expressing heart cells, with each division producing one Svp-CC and one Svp-PC per hemisegment (yellow and red cells respectively in Figure 3A; Gajewski et al., 2000; Ward and Skeath, 2000). In contrast, a pair of symmetric cell divisions gives rise to the four Tin-CCs in each hemisegment, the two Tin-Lb-CCs and the two posterior-most Tin-CCs (green cells in Figure 3A; Han and Bodmer, 2003). These lineage relationships are shown in Figure 3G.

We took advantage of this ability to distinguish the products of asymmetric and symmetric cardiac progenitor cell divisions to determine whether cell division defects are responsible for the heart phenotypes seen in *jumu* and *CHES-1-like* mutants. Indeed, one source of the localized increase in CC number in embryos lacking *jumu* or *CHES-1-like* function is an abnormal asymmetric cell division that causes a Svp progenitor cell to yield two Svp-CCs instead of one Svp-CC and one Svp-PC (phenotype I in Figures 3B, 3F and 3G). Conversely, in some cases a Svp progenitor produces two Svp-PCs instead of a Svp-CC and

a Svp-PC, resulting in a localized reduction in CC number in *jumu* mutants (phenotype II in Figures 3B and 3G).

Occasional karyokinesis defects also occurred during the asymmetric division of Svp progenitor cells in both *jumu* and *CHES-1-like* mutants (phenotype III in Figures 3C, 3F and 3G). This finding is more clearly illustrated in a three-dimensional reconstruction of microscopic images corresponding to the two highlighted opposing hemisegments in Figure 3C (also see Movie S1). Note that the posterior-most Svp-CC nuclei in each hemisgment are arrested in the process of dividing, with each appearing to possess two nuclei that are unable to completely dissociate. The karyokinesis defects did not change the number of Svp-CCs, but there was a reduction in the number of associated Svp-PCs. In addition, depending on when the karyokinesis arrest occurred, some of the Svp-CC nuclei appeared larger than normal. Mutations in *jumu* and *CHES-1-like* also caused karyokinesis defects in the symmetrically dividing Tin-CCs, which resulted in a localized reduction in the number of these cells (phenotype IV in Figures 3C, 3D, 3F and 3G).

We also observed localized increases in the number of Tin-CCs in *jumu* and *CHES-1-like* mutant embryos (phenotype V in Figures 3D, 3F and 3G). Additional cell division is the likely source of these extra Tin-CCs since in mutant embryos some hemisegments had wild-type numbers of Svp-CCs and Tin-CCs but one or more Tin-CCs were arrested in the process of undergoing extra cell division (Figure 3E).

Finally, a small fraction of hemisegments in both *jumu* null and *CHES-1-like* null mutant hearts exhibit two phenotypes which cannot be explained by any of the previously considered mechanisms: (i) hemisegments containing only one Svp-CC and one Svp-PC (Figure S3A-S3B), and (ii) hemisegments with a total of six Svp-expressing cells (Figure S3C-S3D). Defects in the earlier round of cell divisions that give rise to the Svp progenitors can explain both of these phenotypes. In the first case, this mechanism would produce only one Svp progenitor cell in a hemisegment—which, in turn, could give rise to only two Svp heart cells—and in the second case, it would generate three Svp progenitor cells which subsequently divide to yield six Svp cardiac cells. A quantitative summary of the *jumu* and *CHES-1-like* mutant phenotypes, the statistical significance of each class, and the mechanisms by which they arise are found in Tables S2A-S2B.

Figures 3D and 3F illustrate one possible reason for incorrectly positioned CCs in *jumu* and *CHES-1-like* mutants. When one hemisegment contains as many as eight CCs, and its counterpart across the dorsal midline has as few as five such cells, keeping the hemisegments aligned requires one of the rows of CCs to bulge out (Figure 2G). Alternatively, some of the excess CCs may be displaced from their normal linear arrangement (Figures 3D and 3F). This latter model is supported by the observation that, in *jumu* and *CHES-1-like* mutants, segments in which opposing hemisegments have unequal numbers of CCs exhibit significantly more incorrectly positioned cells than do segments with hemisegments containing the same number of CCs (Tables S2C-S2D).

In summary, all of the heart phenotypes observed in *jumu* and *CHES-1-like* mutants can be accounted for by defects in different aspects of the asymmetric or symmetric division of cardiac progenitor cells.

Asymmetric cell division defects in *jumu* and *CHES-1-like* mutants are a consequence of defective Numb protein localization in Svp cardiac progenitor cells

Membrane-associated Numb protein localizes on one side of asymmetrically dividing neural precursor cells and segregates to only one of the two daughter cells where it antagonizes the activity of Notch, leading to differences in progeny cell fates (Rhyu et al., 1994; Spana and

Doe, 1996). Although Numb expression has not previously been examined in Svp cardiac progenitor cells, the identification of supernumerary Svp-PCs in *numb* mutants was used in a prior study to infer that *numb* plays a similar role in the Svp progenitors, with the daughter cell which inherits most of Numb protein assumed to adopt a Svp-CC fate (Ward and Skeath, 2000). We pursued this hypothesis in more detail by both genetic interaction and Numb protein localization experiments.

If the Svp progenitor cell division defects in *jumu* and *CHES-1-like* mutants is a consequence of the wild-type functions of these genes being mediated via Numb localization during asymmetric cell division, then strong pairwise genetic interactions should occur between *numb* and each of *jumu* and *CHES-1-like* alleles. To examine this possibility, the heart phenotypes of single mutant heterozygotes of these three genes were quantitated and compared with those of embryos that are doubly heterozygous either for mutations in both *jumu* and *numb*, or for mutations in both *CHES-1-like* and *numb* (Figures 4A-4B and Tables S2A-S2B). Double heterozygotes for both *jumu* and the *numb* null mutations exhibit asymmetric cell division defects in Svp-expressing cells that are significantly more severe ($p = 0.0018$) than the additive effects of each of the two single heterozygotes. In contrast, defects in the symmetric cell divisions that yield the Tin-CCs in the double heterozygotes are not significantly different ($p = 0.7198$) from the additive effects of the single *jumu* and *numb* heterozygotes. A similar synergistic genetic interaction between *CHES-1-like* and *numb* occurs for asymmetric ($p = 0.0124$) but not for symmetric ($p = 0.5863$) cardiac cell divisions. Together, these results are consistent with *jumu* and *CHES-1-like* acting through *numb* to regulate the asymmetric cell division of Svp cardiac progenitor cells.

To directly test whether Numb mislocalization is associated with *jumu* and *CHES-1-like* mutant cardiac cell fate phenotypes, we first stained wild-type embryos carrying the *svp-lacZ* enhancer trap for expression of both Numb and β-galactosidase. Numb protein is asymmetrically localized in a crescent at one pole of normal Svp progenitor cells (Figure 4C). Thus, only one of the two daughter cells should inherit most of this protein and adopt a Svp-CC fate.

In contrast, in embryos homozygous for single or double null mutations of *jumu* and *CHES-1-like*, Numb protein is found in a more diffuse halo surrounding most of the nuclei in all dividing Svp progenitor cells (Figure 4D-4F). This finding implies that, after cell division, both progeny cells inherit roughly equal amounts of Numb protein, resulting in an inability to distinguish one cell from the other and with both taking on the same fate. Of note, similar Numb localization defects are also detected in some dividing Svp progenitor cells from embryos doubly heterozygous for mutations in the Fkh genes and *numb*, but not in *numb* heterozygotes (Figure 4G-4J).

Proper asymmetric localization of Numb protein in the Svp progenitor cells during asymmetric cell division requires its physical interaction and colocalization with phosphorylated Partner of Numb (Pon) protein (Lu et al., 1998; Wang et al., 2007). Intriguingly, synergistic genetic interactions are also observed between *jumu* and *pon*, and between *CHES-1-like* and *pon*, during asymmetric, but not during symmetric, cell divisions of the Svp progenitor cells (Figures 4K-4L and Tables S2A-S2B). These findings suggest that the utilization of *numb* by *jumu* and *CHES-1-like* during asymmetric cell division also involves *pon* function.

Loss of *polo* function phenocopies the cardiac defects of *jumu* and *CHES-1-like* mutants

The requirement of both *jumu* and *CHES-1-like* for the proper localization of Numb during the asymmetric cell division of cardiac progenitors led us to consider that other regulators of mitosis might be involved in the effects of these Fkh transcription factors. One plausible

candidate is *polo*, which encodes a kinase that phosporylates Pon, the protein that serves as an adapter for Numb during its asymmetric cellular localization (Wang et al., 2007), and which, as noted previously, exhibits synergistic genetic interactions with both *jumu* and *CHES-1-like* during asymmetric division of Svp cardiac progenitors. Intriguingly, Polo kinase not only regulates asymmetric cell division but also has been implicated in multiple steps of mitosis, meiosis and cytokinesis (Archambault and Glover, 2009), observations that correlate with the other *jumu* and *CHES-1-like* mutant cardiac phenotypes. Furthermore, a *polo* ortholog plays a role in cardiac myocyte proliferation during zebrafish heart regeneration (Jopling et al., 2010). Of additional significance, *polo* ranked very highly in our statistical meta-analysis for identifying genes expressed in the CM (rank position 66; Table S1A). Moreover, in situ hybridization revealed that the *polo* transcript is indeed transiently detected in the CM during embryonic stages 11 to 12 when cardiac progenitor cells divide (Figure 5A).

To test the hypothesis that *jumu* and *CHES-1-like* function in heart development by a *polo*-mediated pathway, we initially examined the cardiac expression of Mef2 in *polo* mutants. Embryos homozygous for either of two strong *polo* hypomorphic mutations, $polo^{9}$ and $polo^{10}$ (Donaldson et al., 2001), exhibit localized increases or decreases in Mef2-positive CC number, larger than normal CC nuclei and incorrectly positioned CCs (Figures 5B-5D), all of which phenocopy *jumu* and *CHES-1-like* mutants. Furthermore, the same five classes of cell division defects as previously described for *jumu* and *CHES-1-like* mutants occur with *polo* loss-of-function (Figures 5E-5I and Table S2A). These observations suggest that *jumu* and *CHES-1-like* act through a *polo*-mediated pathway to regulate the division and fates of cardiac progenitor cells, a possibility that we examined with the following series of additional experiments.

Synergistic genetic interactions between *jumu*, *CHES-1-like* and *polo*

If *jumu, CHES-1-like* and *polo* function together during cardiogenesis, they might exhibit strong genetic interactions. To assess this possibility, the heart phenotypes of single heterozygotes for mutations in each of these three genes were quantitated and compared with those of embryos that are doubly heterozygous for mutations in all pairwise combinations of these genes. Our results (Figures 6A-6B and S4A, Tables S2A-S2B) demonstrated that synergistic genetic interactions indeed occur between *jumu* and *polo*, between *CHES-1-like* and *polo*, and between *jumu* and *CHES-1-like* during both asymmetric and symmetric cell divisions, suggesting that all three genes regulate heart development by functioning together in the same genetic pathway. Consistent with this model, many of the dividing Svp progenitor cells in these double heterozygotes also exhibit defective Numb localization (Figures 4J and 6E-6F).

Polo protein fails to localize at centrosomes of dividing cardiac progenitors in *jumu* and *CHES-1-like* mutants

We next considered the possibility that mutations in *jumu* and *CHES-1-like* might alter the expression level or subcellular distribution of Polo kinase. Since Polo normally localizes at the centrosomes of mitotically dividing cells where it is required for proper spindle assembly (Archambault and Glover, 2009; Moutinho-Santos et al., 1999), whether Jumu and CHES-1-like affect Polo protein can be assessed by determining if there are centrosomes lacking Polo in dividing cardiac cells that are mutant for *jumu* and *CHES-1-like*. Thus, we simultaneously stained wild-type and appropriate mutant embryos containing a *svp-lacZ* enhancer trap with antibodies against β-galactosidase (to detect Svp progenitor cells), phospho-histone H3 (to detect dividing cells), Pericentrin-like protein (PLP, a centriole/centrosome marker), and Polo.

In all 15 of the dividing wild-type Svp progenitor cells examined, Polo protein co-localized with PLP (Figures 5J-5J'''). In contrast, in 15 dividing Svp progenitor cells in each of *jumu* and *CHES-1-like* null mutant embryos, Polo was not detected at the centrosome in 3 and 2 cells, respectively (Figures 5K-5L'''). The incomplete penetrance of this effect is consistent with the observation that not all cardiac progenitors exhibit cell division defects in these mutants (Figure 3 and Table S2A). The Polo staining results could reflect either a defect in Polo protein localization to centrosomes or an overall reduction in Polo protein level. In either case, our data suggest that Jumu and CHES-1-like act upstream of the mitotic regulatory kinase encoded by *polo*.

Ubiquitously expressed or cardiac mesoderm-targeted *polo* partially rescues both *jumu* and *CHES-1-like* mutant phenotypes

To test the hypothesis that the Fkh genes act upstream of *polo, polo* was expressed under the control of a *ubiquitin* promoter in wild-type embryos and in embryos homozygous for either *jumu* or *CHES-1-like* null mutations. If *polo* acts downstream of the Fkh transcription factors, then ubiquitous expression of *polo* should at least partially rescue the cardiac phenotypes associated with the Fkh gene mutants. While in a control experiment ubiquitous expression of *polo* does not affect heart development in wild-type embryos, ectopic *polo* significantly reduces the severity of the cardiac defects associated with either single Fkh gene mutant alone (Figures 6C-6D and S4B-S4F, Tables S2A-S2B). The effect of ectopic *polo* is so efficient that the hearts in 4 out of 17 and 6 out of 16 of the rescued *jumu* and *CHES-1-like* mutant embryos, respectively, appeared completely wild-type (Figures S4D and S4F). Partial rescue of the Fkh mutant phenotypes was also obtained by driving *polo* expression specifically in the cardiac mesoderm by a *tinD-GAL4* driver (Figures 6C-6D and Tables S2A-S2B), thereby indicating that the requirement of *polo* for correct asymmetric and symmetric cardiac progenitor cell divisions is autonomous to the heart.

The ubiquitous expression of *polo* in either *jumu* or *CHES-1-like* mutants also restored the proper asymmetric localization of Numb protein in some, but not all of the dividing Svp progenitor cells (Figures 6G-6H). Whereas Polo protein was not detected in the centrosomes of a small fraction of the dividing Svp progenitors in either *jumu* or *CHES-1-like* mutants (Figures 5K-5L''), Polo protein was localized in the centrosomes of all 15 of the dividing Svp progenitors that were examined for each Fkh mutant in which *polo* was constitutively expressed under the control of the *ubiquitin* promoter (Figure S4I-S4J''').

Of note, the more severe phenotype in which cardiac cells were entirely missing from some hemisegments in a significant fraction (8/50; $p = 0.00054$) of embryos doubly homozygous for both *jumu* and *CHES-1-like* null mutations could not be rescued by ubiquitous expression of *polo* (11 out of 50 double mutants with the *Ubi-GFP-polo* transgene exhibited similar defects; Figures S4G-S4H). This result suggests that *jumu* and *CHES-1-like* regulate heart development by additional, *polo*-independent mechanisms.

Collectively, the failure to detect Polo in the centrosomes of dividing heart cells in the Fkh gene mutants, and the partial rescue of cardiac phenotypes in both *jumu* and *CHES-1-like* mutants by either ubiquitously expressed or CM-targeted *polo*, argue strongly that both Fkh genes act upstream of *polo* in a regulatory pathway governing cardiac progenitor cell divisions.

Identification of genes putatively upregulated by *jumu* via microarray-based genome-wide RNA expression profiling

A possible explanation for the partial rescue of the cardiac phenotypes of the Fkh gene mutants is that Jumu and CHES-1-like directly or indirectly control the transcription of *polo.*

We tested this hypothesis by overexpressing Jumu throughout the mesoderm with a *twi-Gal4* driver, and by using Affymetrix microarrays to quantitate the effects of this genetic perturbation on *polo* expression levels in stage 11-12 mesodermal cells that were purified by flow cytometry to enrich for mesoderm-specific responses. This strategy offers the additional advantage of simultaneously measuring the transcriptional responses of other mesodermal genes to ectopic *jumu* on a genome-wide scale. Compared to wild-type, *jumu* overexpression is associated with a significantly elevated level of *polo* expression (>1.6-fold enrichment; $p < 0.05$; Table S3A), suggesting that *jumu* indeed activates *polo* transcription.

Furthermore, this genome-wide expression profiling experiment identified a total of 374 genes whose expression levels are significantly elevated when *jumu* is overexpressed in the entire mesoderm (Table S3A). Of note, 24 of the 110 cardiac genes previously described in this study (Table S1) are included among the 374 *jumu*-upregulated genes (Table S3A). This number represents a statistically significant overrepresentation of cardiac genes among those upregulated by *jumu* ($p < 10^{-14}$ by the hypergeometric distribution).

To gain insight into the biological processes in which the *jumu*-upregulated mesodermal genes are involved, this gene set was queried for the relative enrichment of Gene Ontology (GO) terms (Table S3B). The overrepresented GO terms include multiple categories associated with asymmetric and symmetric cell division, cell cycle and cytokinesis, suggesting that the regulation of these processes by Jumu also involves genes independent of but having functions related to that of *polo*. Prominent examples of such potentially synergistically acting Jumu-responsive genes include abnormal spindle, Inner centromere protein, pavarotti and *borealin-related*.

Synergistic interactions between the genes encoding the Jumu and CHES-1-like Fkh proteins and other known cardiogenic transcription factors

The results described above illustrate how the two transcription factors encoded by *jumu* and *CHES-1-like* act through *polo* to ensure that the differentiated heart acquires the requisite types, numbers and arrangement of cardiac cells. Other transcription factors known to play critical early roles in cardiogenesis include the NK homeodomain Tin, the three T-box factors encoded by the *Dorsocross* genes, *Doc1, Doc2* and *Doc3*, and the GATA factor encoded by *pannier* (*pnr*) (Alvarez et al., 2003; Azpiazu and Frasch, 1993; Bodmer, 1993; Reim and Frasch, 2005). Thus, we undertook genetic interaction experiments to determine whether these previously characterized cardiogenic transcription factors also participate in the developmental pathways governed by the Fkh proteins Jumu and CHES-1-like in the heart.

Our results (Tables S2A-S2B) demonstrate synergistic genetic interactions between the Fkh genes and *tin* during both asymmetric and symmetric cell divisions (Figures 7A-7B), synergistic interactions between the *Doc* genes and the Fkh genes only during symmetric cell divisions (Figures 7C-7D), and no genetic interactions between either Fkh gene and *pnr* (Figures 7E-7F). Collectively, these data suggest that *tin* and the Fkh genes act together during both asymmetric and symmetric cell divisions, that the *Doc* genes and the Fkh genes are closely associated only during symmetric cell divisions, and that *pnr* regulates heart development by mechanisms not involving either of the Fkh genes.

DISCUSSION

In this study, we used an integrated strategy to discover genes expressed in a complex organ and its progenitor cells by combining informative genetic perturbations of development, a statistical analysis of the genome-wide gene expression profiles of purified primary cells of interest, and the large-scale validation of predicted gene expression patterns by whole-

embryo in situ hybridization. This approach offers two significant advantages over other studies undertaken to identify genes involved in a particular developmental process. First, isolating the cells of interest eliminates the potentially confounding effects of genetic perturbations in the rest of the embryo and increases the sensitivity of genome-wide expression profiling. Second, by examining perturbations of not one, but multiple convergent developmental pathways, any bias associated with the manipulation of a single genetic pathway is reduced and the relative contribution of each pathway to gene expression is taken into consideration in the statistical meta-analysis, thereby increasing the accuracy of the gene predictions.

The 70 genes found to be expressed in the *Drosophila* CM and differentiated heart by this strategy provide a substantial set of candidates that can be examined for possible roles in cardiac development, as well as in mechanistic studies of gene regulation. Here, we focused on the cardiogenic functions of *jumu* and *CHES-1-like*, both of which encode Fkh transcription factors and function upstream of *polo* to control multiple processes in the developing heart, including both the symmetric and asymmetric division of cardiac progenitors, karyokinesis, cell fate specification and the proper positioning of CCs within the mature heart. The serine-threonine kinase encoded by *Drosophila polo*—and its orthologs in mammals, yeast, frogs and nematodes—are known to play essential roles in a number of conserved biological processes involved in both mitotic and meiotic cell divisions (Archambault and Glover, 2009). These functions include: (1) the initial entry into M phase, a defect in which could yield the karyokinesis phenotype seen in our study; (2) centrosome maturation and spindle formation, defects in which could result in problems with spindle orientation and assembly that might also account for the karyokinesis phenotype, as well as the observed increase in Tin-CCs and abnormalities in cell positioning; (3) determination of cell fates during asymmetric cell division by the Polo-mediated phosphorylation of Pon, errors in which could generate improper sibling identities in the progeny of the Svp progenitor cell; and (4) exit out of mitosis and the promotion of cytokinesis, flaws in which could additionally explain the karyokinesis abnormality. Of note, spindle assembly problems are also seen with loss-of-function of *jumu* and *CHES-1-like* in *Drosophila* S2 cells (Goshima et al., 2007). Thus, failure to correctly regulate the activity of the downstream gene *polo* could explain the entirety of the cardiac phenotypes that occur in *jumu* and *CHES-1-like* single mutant embryos. In contrast, the severity of the double compared with the single mutant *jumu* and *CHES-1-like* cardiac phenotypes, and the results of the *polo* rescue experiments, suggest that partially redundant *polo*-independent pathways must also regulate the cardiogenic functions of these two Fkh factors.

Given current knowledge about Polo function, there are at least three mechanisms by which *polo* activity could be controlled by Jumu and CHES-1-like. First, since Polo kinase is known to be activated by phosphorylation of its T-loop (Jang et al., 2002; Qian et al., 1999), the Fkh factors could affect this regulatory step. We do not favor this mechanism since mutations in either Fkh gene affect localization of Polo protein at centrosomes and/or the level of Polo protein, and either ubiquitous or CM-targeted *polo* expression rescues *jumu* and *CHES-1-like* mutants. Second, Jumu and CHES-1-like could influence the well-established Ubiquitin-dependent proteolysis of Polo (Lindon and Pines, 2004). In this context, it is worth noting that absence of COP9 complex homolog subunit 4, a member of a protein complex regulating Ubiquitin-mediated protein degradation, exhibits similar cardiac phenotypes as those observed for loss of *jumu*, *CHES-1-like* and *polo* functions (Tao et al., 2007). Further experiments will be required to assess whether the *Drosophila* Fkh transcription factors regulate such a pathway.

A third alternative is that Jumu and CHES-1-like directly or indirectly control the transcription of *polo*. The observation that Fkh transcription factors are required for the

expression of *polo* orthologs in other species (Buck et al., 2004; Laoukili et al., 2005; Zhu et al., 2000) is consistent with the possibility that *jumu* and *CHES-1-like* could have a similar regulatory effect in *Drosophila*. We found additional evidence supporting this hypothesis through our determination that *polo* expression levels are appreciably increased when *jumu* is ectopically over-expressed throughout the entire mesoderm, and that other genes having functions related to *polo* are similary upregulated by ectopic Jumu. Furthermore, chromatin immunoprecipitation data from the modENCODE project (Negre et al., 2011) indicate that Jumu protein binds to the *polo* genomic region during the stage of embryogenesis when the CM develops, suggesting that this Fkh transcription factor might directly control *polo* transcription in cardiac progenitor cells.

The observation that FoxM1, a subclass M Fkh protein, transcriptionally regulates a *polo* ortholog in mammalian cell lines (Laoukili et al., 2005) is also of interest since *FoxM1* homozygous knockout mice die in the perinatal period with dilated hearts (Korver et al., 1998). Moreover, histological analysis shows that the orientation of cardiomyocytes in *FoxM1* mutant hearts is highly irregular, and the nuclei of these cardiomyocytes are enlarged, consistent with being polyploid (Korver et al., 1998). These phenotypes of *FoxM1* mutant mice are remarkably similar to those of *jumu* and *CHES-1-like* mutants in *Drosophila*, suggesting that the cardiogenic roles of both Fkh genes and *polo* have been evolutionarily conserved.

In summary, our genetic analysis of the roles played by two mesodermally expressed Fkh transcription factors in mediating Polo-dependent cardiac progenitor cell divisions, our characterization of numerous *jumu*-responsive mesodermal genes, and the interactions we uncovered between the Fkh proteins Jumu and CHES-1-like and other classes of cardiogenic transcription factors emphasize the elaborate architecture of the regulatory network that is required for the precise orchestration of multiple developmental events during the formation of an organ comprising multiple differentiated cell types. Furthermore, the present findings illustrate how the coordination of diverse biological processes is achieved during development of the *Drosophila* embryonic heart through the localized control of a ubiquitous cell cycle regulator by the spatially and temporally restricted activities of two Fkh transcription factors.

EXPERIMENTAL PROCEDURES

Fluorescence activated cell sorting and gene expression profiling

Microarray-based gene expression profiles for GFP-positive and GFP-negative cells isolated by fluorescence-activated sorting of a single cell suspension prepared from homozygous *tinD-GFP* stage 11 embryos were obtained as described previously (Estrada et al., 2006). These data were combined with prior microarray results derived for the 9 genetic perturbations shown in Figure 1E (Estrada et al., 2006) in order to facilitate the cardiac meta-analysis undertaken in this study.

The statistical methods for combining multiple related microarray datasets to predict genes with expression similar to a training set of known co-expressed genes has previously been described in detail (Estrada et al., 2006). In brief, each gene is assigned a “combined significance statistic” T which is the weighted sum of the CyberT t-statistics for that gene from each condition-to-control comparison performed, as calculated using the Goldenspike R package (Choe et al., 2005) and multiplied by a “sign” term (1 or −1) reflecting the expected direction of change in expression of target genes in a given genetic condition. Weight profiles are systematically assessed for the ability to detect genes from the training set among the top-ranked genes at a variety of q-value cutoffs; those combinations of weights that were among the top 10% at all cutoffs examined were averaged to produce the

final combination of weights used to generate the *T* scores on which genes were ultimately ranked (Figures 1F-1H).

Microarray-based gene expression profiles for GFP-positive cells isolated by fluorescence-activated sorting of single cell suspensions prepared from stage 11-12 *twi-GAL4 UAS-2EGFP/UAS-jumu* embryos and stage 11-12 *twi-GAL4 UAS-2EGFP* embryos were also obtained by Affymetrix microarray hybridization. These array data were analyzed using the *affy* (Gautier et al., 2004) and *limma* (Smyth, 2004) Bioconductor package. Raw intensities were normalized separately using the mas5 and rma commands with default settings; linear models were fitted separately to each normalized dataset in *limma*. Probesets were filtered for $\log_2$(fold change) > 0.5 and adjusted p-value < 0.1 after correction for multiple hypothesis testing, and only those genes represented by probesets meeting both criteria in both tests were considered further (Table S3).

Generation of a *CHES-1-like* deficiency strain

CHES-1-like was deleted by FLP-catalyzed recombination (Parks et al., 2004) using the FRT-containing transposons e02377 and e04245 that flank the gene (Thibault et al., 2004). The absence of the gene in the resulting deficiency, *Df(1)CHES-1-like*^{1}, was confirmed by PCR analysis (Figure S2). Homozygotes and hemizygotes for *Df(1)CHES-1-like*^{1} are viable and fertile, but every mutant embryo exhibits the heart phenotypes described in this study.

At the time that the targeted deletion strategy was designed and the crosses were undertaken, *CHES-1-like* was the only known gene that was predicted to be deleted. However, a more recent annotation of the *Drosophila* genome places another gene of unknown function, *CG43287*, in the deleted interval. While we cannot rule out a contribution of this second gene to the mutant phenotype associated with *Df(1)CHES-1-like*^{1}, the similarity between the CHES-1-like RNAi and *Df(1)CHES-1-like*^{1} heart phenotypes strongly suggests that loss of *CHES-1-like* function is the primary cause of the cardiac defects.

RNAi assays

Whole embryo RNAi assays were performed as previously described (Estrada et al., 2006). RNAi assays targeted to specific embryonic cell types were carried out by expressing the UAS-inverted repeat constructs GD4099 (*jumu* dsRNA) and KK101264 (*CHES-1-like* dsRNA) (Dietzl et al., 2007) in the cardiac mesoderm using both the *tinD-GAL4* and *Hand-GAL4* drivers simultaneously. Mef2-stained hearts of stage 16 embryos with the genotypes *UAS-Dcr-2; Hand-GAL4/jumu*^{GD4099}*; tinD-GAL4/+* and UAS-Dcr-2; Hand-GAL4/ CHES-1-like^{KK101264}; tinD-GAL4/+ raised at 29°C were compared with those of siblings lacking the inverted repeat constructs as negative controls.

Enrichment of Gene Ontology terms

The FuncAssociate 2.0 web application (Berriz et al., 2009) was utilized to query for relative enrichment of Gene Ontology terms both in genes identified as being expressed in the CM or heart and in genes with elevated expression levels when *jumu* was ectopically expressed throughout the entire mesoderm.

Supplementary Material

Refer to Web version on PubMed Central for supplementary material.

Acknowledgments

We thank A. Hofmann, B. Paterson, B. Durand, J. B. Skeath, B. Lu, R. S. Hawley, Y. Xiaohang, I. Reim, Z. Han, J. Lipsick, the Bloomington *Drosophila* Stock Center, the Exelixis Collection at the Harvard Medical School, the Vienna *Drosophila* RNAi Center and the Developmental Studies Hybridoma Bank for fly lines and reagents; Y. Kim and X. Zhu for helpful discussions; G. C. Rogers for technical assistance with Polo antibody production; and C. Sonnenbrot, L. Phun and the NHLBI Flow Cytometry and Gene Expression Core Facilities for assistance with experiments. This work was supported by the NHLBI Division of Intramural Research (A.M.M. and N.M.R.) and by an American Heart Association Postdoctoral Fellowship (S.M.A.).

REFERENCES

Alvarez AD, Shi W, Wilson BA, Skeath JB. pannier and pointedP2 act sequentially to regulate Drosophila heart development. Development. 2003; 130:3015–3026. [PubMed: 12756183]

Archambault V, Glover DM. Polo-like kinases: conservation and divergence in their functions and regulation. Nat Rev Mol Cell Biol. 2009; 10:265–275. [PubMed: 19305416]

Azpiazu N, Frasch M. tinman and bagpipe: two homeo box genes that determine cell fates in the dorsal mesoderm of Drosophila. Genes Dev. 1993; 7:1325–1340. [PubMed: 8101173]

Berriz GF, Beaver JE, Cenik C, Tasan M, Roth FP. Next generation software for functional trend analysis. Bioinformatics. 2009; 25:3043–3044. [PubMed: 19717575]

Bodmer R. The gene tinman is required for specification of the heart and visceral muscles in Drosophila. Development. 1993; 118:719–729. [PubMed: 7915669]

Bodmer, R.; Frasch, M. Development and Aging of the Drosophila Heart. In: Rosenthal, N.; Harvey, RP., editors. Heart Development and Regeneration. Academic Press; London, UK: 2010. p. 47-86.

Bryantsev AL, Cripps RM. Cardiac gene regulatory networks in Drosophila. Biochim Biophys Acta. 2009; 1789:343–353. [PubMed: 18849017]

Buck V, Ng SS, Ruiz-Garcia AB, Papadopoulou K, Bhatti S, Samuel JM, Anderson M, Millar JB, McInerny CJ. Fkh2p and Sep1p regulate mitotic gene transcription in fission yeast. J Cell Sci. 2004; 117:5623–5632. [PubMed: 15509866]

Carmena A, Gisselbrecht S, Harrison J, Jimenez F, Michelson AM. Combinatorial signaling codes for the progressive determination of cell fates in the Drosophila embryonic mesoderm. Genes Dev. 1998; 12:3910–3922. [PubMed: 9869644]

Cheah PY, Chia W, Yang X. Jumeaux, a novel Drosophila winged-helix family protein, is required for generating asymmetric sibling neuronal cell fates. Development. 2000; 127:3325–3335. [PubMed: 10887088]

Chien KR, Domian IJ, Parker KK. Cardiogenesis and the complex biology of regenerative cardiovascular medicine. Science. 2008; 322:1494–1497. [PubMed: 19056974]

Choe SE, Boutros M, Michelson AM, Church GM, Halfon MS. Preferred analysis methods for Affymetrix GeneChips revealed by a wholly defined control dataset. Genome Biol. 2005; 6:R16. [PubMed: 15693945]

Dietzl G, Chen D, Schnorrer F, Su KC, Barinova Y, Fellner M, Gasser B, Kinsey K, Oppel S, Scheiblauer S, et al. A genome-wide transgenic RNAi library for conditional gene inactivation in Drosophila. Nature. 2007; 448:151–156. [PubMed: 17625558]

Donaldson MM, Tavares AA, Ohkura H, Deak P, Glover DM. Metaphase arrest with centromere separation in polo mutants of Drosophila. J Cell Biol. 2001; 153:663–676. [PubMed: 11352929]

Estrada B, Choe SE, Gisselbrecht SS, Michaud S, Raj L, Busser BW, Halfon MS, Church GM, Michelson AM. An integrated strategy for analyzing the unique developmental programs of different myoblast subtypes. PLoS Genet. 2006; 2:e16. [PubMed: 16482229]

Frasch M. Induction of visceral and cardiac mesoderm by ectodermal Dpp in the early Drosophila embryo. Nature. 1995; 374:464–467. [PubMed: 7700357]

Gajewski K, Choi CY, Kim Y, Schulz RA. Genetically distinct cardial cells within the Drosophila heart. Genesis. 2000; 28:36–43. [PubMed: 11020715]

Gautier L, Cope L, Bolstad BM, Irizarry RA. affy--analysis of Affymetrix GeneChip data at the probe level. Bioinformatics. 2004; 20:307–315. [PubMed: 14960456]

Gisselbrecht S, Skeath JB, Doe CQ, Michelson AM. heartless encodes a fibroblast growth factor receptor (DFR1/DFGF-R2) involved in the directional migration of early mesodermal cells in the Drosophila embryo. Genes Dev. 1996; 10:3003–3017. [PubMed: 8957001]

Goshima G, Wollman R, Goodwin SS, Zhang N, Scholey JM, Vale RD, Stuurman N. Genes required for mitotic spindle assembly in Drosophila S2 cells. Science. 2007; 316:417–421. [PubMed: 17412918]

Grigorian M, Mandal L, Hakimi M, Ortiz I, Hartenstein V. The convergence of Notch and MAPK signaling specifies the blood progenitor fate in the Drosophila mesoderm. Dev Biol. 2011; 353:105–118. [PubMed: 21382367]

Han Z, Bodmer R. Myogenic cells fates are antagonized by Notch only in asymmetric lineages of the Drosophila heart, with or without cell division. Development. 2003; 130:3039–3051. [PubMed: 12756185]

Han Z, Olson EN. Hand is a direct target of Tinman and GATA factors during Drosophila cardiogenesis and hematopoiesis. Development. 2005; 132:3525–3536. [PubMed: 15975941]

Hartenstein AY, Rugendorff A, Tepass U, Hartenstein V. The function of the neurogenic genes during epithelial development in the Drosophila embryo. Development. 1992; 116:1203–1220. [PubMed: 1295737]

Jagla K, Frasch M, Jagla T, Dretzen G, Bellard F, Bellard M. ladybird, a new component of the cardiogenic pathway in Drosophila required for diversification of heart precursors. Development. 1997; 124:3471–3479. [PubMed: 9342040]

Jang YJ, Ma S, Terada Y, Erikson RL. Phosphorylation of threonine 210 and the role of serine 137 in the regulation of mammalian polo-like kinase. J Biol Chem. 2002; 277:44115–44120. [PubMed: 12207013]

Jopling C, Sleep E, Raya M, Marti M, Raya A, Belmonte JC. Zebrafish heart regeneration occurs by cardiomyocyte dedifferentiation and proliferation. Nature. 2010; 464:606–609. [PubMed: 20336145]

Korver W, Schilham MW, Moerer P, van den Hoff MJ, Dam K, Lamers WH, Medema RH, Clevers H. Uncoupling of S phase and mitosis in cardiomyocytes and hepatocytes lacking the winged-helix transcription factor Trident. Curr Biol. 1998; 8:1327–1330. [PubMed: 9843684]

Laoukili J, Kooistra MR, Bras A, Kauw J, Kerkhoven RM, Morrison A, Clevers H, Medema RH. FoxM1 is required for execution of the mitotic programme and chromosome stability. Nat Cell Biol. 2005; 7:126–136. [PubMed: 15654331]

Lee HH, Frasch M. Survey of forkhead domain encoding genes in the Drosophila genome: Classification and embryonic expression patterns. Dev Dyn. 2004; 229:357–366. [PubMed: 14745961]

Lindon C, Pines J. Ordered proteolysis in anaphase inactivates Plk1 to contribute to proper mitotic exit in human cells. J Cell Biol. 2004; 164:233–241. [PubMed: 14734534]

Lu B, Rothenberg M, Jan LY, Jan YN. Partner of Numb colocalizes with Numb during mitosis and directs Numb asymmetric localization in Drosophila neural and muscle progenitors. Cell. 1998; 95:225–235. [PubMed: 9790529]

Mandal L, Banerjee U, Hartenstein V. Evidence for a fruit fly hemangioblast and similarities between lymph-gland hematopoiesis in fruit fly and mammal aorta-gonadal-mesonephros mesoderm. Nat Genet. 2004; 36:1019–1023. [PubMed: 15286786]

Michelson AM, Gisselbrecht S, Zhou Y, Baek KH, Buff EM. Dual functions of the heartless fibroblast growth factor receptor in development of the Drosophila embryonic mesoderm. Dev Genet. 1998; 22:212–229. [PubMed: 9621429]

Moutinho-Santos T, Sampaio P, Amorim I, Costa M, Sunkel CE. In vivo localisation of the mitotic POLO kinase shows a highly dynamic association with the mitotic apparatus during early embryogenesis in Drosophila. Biol Cell. 1999; 91:585–596. [PubMed: 10629938]

Negre N, Brown CD, Ma L, Bristow CA, Miller SW, Wagner U, Kheradpour P, Eaton ML, Loriaux P, Sealfon R, et al. A cis-regulatory map of the Drosophila genome. Nature. 2011; 471:527–531. [PubMed: 21430782]

Parks AL, Cook KR, Belvin M, Dompe NA, Fawcett R, Huppert K, Tan LR, Winter CG, Bogart KP, Deal JE, et al. Systematic generation of high-resolution deletion coverage of the Drosophila melanogaster genome. Nat Genet. 2004; 36:288–292. [PubMed: 14981519]

Qian YW, Erikson E, Maller JL. Mitotic effects of a constitutively active mutant of the Xenopus polo-like kinase Plx1. Mol Cell Biol. 1999; 19:8625–8632. [PubMed: 10567586]

Reim I, Frasch M. The Dorsocross T-box genes are key components of the regulatory network controlling early cardiogenesis in Drosophila. Development. 2005; 132:4911–4925. [PubMed: 16221729]

Rhyu MS, Jan LY, Jan YN. Asymmetric distribution of numb protein during division of the sensory organ precursor cell confers distinct fates to daughter cells. Cell. 1994; 76:477–491. [PubMed: 8313469]

Rosenthal, N.; Harvey, RP. Heart Development and Regeneration. Academic Press; London, UK: 2010.

Smyth GK. Linear models and empirical bayes methods for assessing differential expression in microarray experiments. Stat Appl Genet Mol Biol. 2004; 3 Article3.

Spana EP, Doe CQ. Numb antagonizes Notch signaling to specify sibling neuron cell fates. Neuron. 1996; 17:21–26. [PubMed: 8755475]

Staehling-Hampton K, Hoffmann FM, Baylies MK, Rushton E, Bate M. dpp induces mesodermal gene expression in Drosophila. Nature. 1994; 372:783–786. [PubMed: 7997266]

Strodicke M, Karberg S, Korge G. Domina (Dom), a new Drosophila member of the FKH/WH gene family, affects morphogenesis and is a suppressor of position-effect variegation. Mech Dev. 2000; 96:67–78. [PubMed: 10940625]

Tao Y, Christiansen AE, Schulz RA. Second chromosome genes required for heart development in Drosophila melanogaster. Genesis. 2007; 45:607–617. [PubMed: 17941041]

Thibault ST, Singer MA, Miyazaki WY, Milash B, Dompe NA, Singh CM, Buchholz R, Demsky M, Fawcett R, Francis-Lang HL, et al. A complementary transposon tool kit for Drosophila melanogaster using P and piggyBac. Nat Genet. 2004; 36:283–287. [PubMed: 14981521]

Wang H, Ouyang Y, Somers WG, Chia W, Lu B. Polo inhibits progenitor self-renewal and regulates Numb asymmetry by phosphorylating Pon. Nature. 2007; 449:96–100. [PubMed: 17805297]

Ward EJ, Skeath JB. Characterization of a novel subset of cardiac cells and their progenitors in the Drosophila embryo. Development. 2000; 127:4959–4969. [PubMed: 11044409]

Yin Z, Xu XL, Frasch M. Regulation of the twist target gene tinman by modular cis-regulatory elements during early mesoderm development. Development. 1997; 124:4971–4982. [PubMed: 9362473]

Zhu G, Spellman PT, Volpe T, Brown PO, Botstein D, Davis TN, Futcher B. Two yeast forkhead genes regulate the cell cycle and pseudohyphal growth. Nature. 2000; 406:90–94. [PubMed: 10894548]

HIGHLIGHTS

- A genomic screen identifies 70 genes expressed in *Drosophila* cardiac cells.
- Two forkhead genes, *jumu* and *CHES-1-like*, regulate *Drosophila* cardiogenesis.
- Symmetric and asymmetric cardiac cell divisions require *jumu* and *CHES-1-like*.
- The cardiogenic effects of *jumu* and *CHES-1-like* are mediated by Polo kinase.

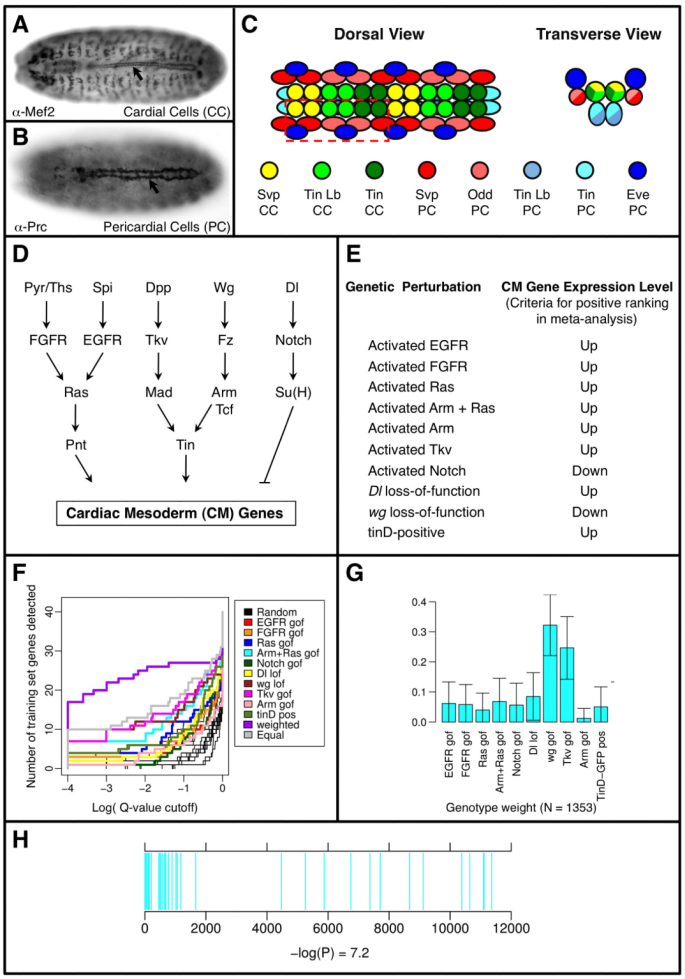

Figure 1. Strategy for gene expression profiling of the *Drosophila* embryonic heart

(A) Staining for expression of Mef2 protein reveals the cardial cells (CCs, arrow) in the heart of a stage 16 embryo.

(B) Staining for expression of Pericardin (Prc) protein reveals the pericardial cells (PCs, arrow) in the heart of a stage 16 embryo.

(C) Schematic diagram showing the stereotyped positions of the 8 different cell types composing the *Drosophila* embryonic heart. An individual hemisegment is indicated by the dashed red box.

(D) Regulatory network responsible for the development of the cardiac mesoderm and heart (Bodmer and Frasch, 2010; Bryantsev and Cripps, 2009).

(E) Genetic perturbations used for gene expression profiling, along with the expected changes in cardiac mesoderm gene levels relative to wild-type mesoderm. “tinD-positive” represents dorsal mesodermal cells isolated from wild-type embryos using targeted expression of GFP driven by the tinD enhancer (Yin et al., 1997).

(F) Detection curves showing the number of genes from the training set detected as a function of q-value cutoff. The predictive value of individual genotype/wild-type comparisons (various colors; see legend) are compared to randomly generated rankings (thin black lines) and to composite rankings derived from a uniform (grey) or a weighted (violet) combination of all datasets.

(G) Weight factors that reflect the relative contribution of each condition (isolated whole mesoderm for 9 genotypes plus purified wild-type tinD-positive cells) to the detection rate of the genes from the training set.
(H) All genes were ranked according to their degree of CM-like expression patterns across the entire set of conditions, using their weighted T-scores. The ranks of the training set genes (blue) are plotted as thin vertical lines, revealing the extent to which optimization concentrates the training set at the top of the rank list. The P-value is from the Wilcoxon-Mann-Whitney *U* test.
See also Figure S1 and Table S1.

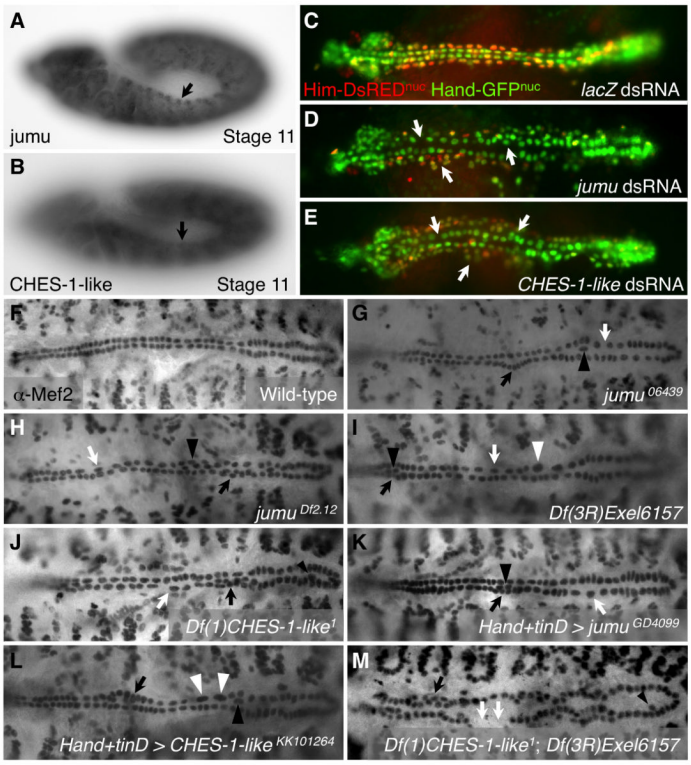

Figure 2. *jumu* and *CHES-1-like* embryonic expression and loss-of-function cardiac phenotypes

(A, B) *jumu* (A) and *CHES-1-like* (B) mRNAs are expressed in the cardiac mesoderm at embryonic stage 11 (arrows).

(C-E) Whole embryo RNAi results for dsRNA corresponding to *lacZ* (C), *jumu* (D), and *CHES-1-like* (E) in live embryos in which CCs express a nuclear localized form of GFP under control of a Hand enhancer (Han and Olson, 2005), and PCs express both Hand-GFP^{nuc} and a nuclear form of DsRed under control of a heart enhancer from the *Him* gene (Him-DsRED^{nuc}; S. Michaud and A.M.M., unpublished results). Arrows indicate incorrect numbers and uneven distribution of CCs and PCs.

(F-M) Mef-2 antibody staining of CCs in wild-type embryos (F), in embryos homozygous for hypomorphic *jumu* mutations (G-H), a *jumu* null deficiency (I), a *CHES-1-like* null mutation (J), in embryos with CM-targeted RNAi against *jumu* (K) and *CHES-1-like* (L), and in embryos homozygous for both the *jumu* and *CHES-1-like* null mutations (M). Localized increases in CC number (black arrows), localized reductions in CC number (white arrows), incorrectly positioned CCs (black arrowheads), CC nuclei larger than normal (white arrowhead), and hemisegments missing all CCs (twin white arrows) are shown.

See also Figure S2.

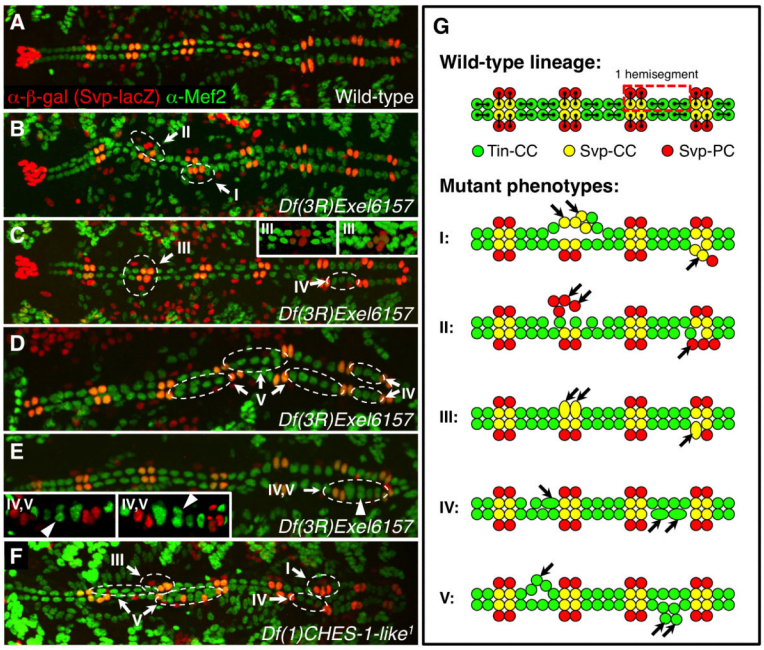

Figure 3. Cell division defects underlying the cardiac phenotypes of *jumu* and *CHES-1-like* mutants

(A) Heart from an otherwise wild-type embryo bearing the *svp-lacZ* enhancer trap showing Tin-CCs (green), Svp-CCs (yellow), and Svp-PCs (red).

(B-F) Hearts from embryos that are homozygous for either the *jumu* null deficiency (B-E) or the *CHES-1-like* null mutation (F), demonstrating cell division defects that underlie the cardiac phenotypes shown in Figure 2. Mutant hemisegments are indicated by dashed ovals, with the Roman numerals corresponding to those in the schematic diagram in panel G. Insets in panel C (different perspectives from a 3D reconstruction) show that each of the posterior Svp-CCs in the highlighted segment demonstrating mutant phenotype III consist of two nuclei that failed to dissociate. See also Movie S1. Similarly, insets in panel E (different perspectives from a 3D reconstruction) show that the highlighted hemisegment contains four Tin-CCs, with one of the Tin-CCs (arrowhead) consisting of two nuclei that failed to dissociate during additional symmetric cell division (mutant phenotypes IV and V).

(G) Schematic showing cell lineage relationships in a wild-type heart and the different cell division defects responsible for the *jumu* and *CHES-1-like* cardiac phenotypes.

See also Figure S3 and Table S2.

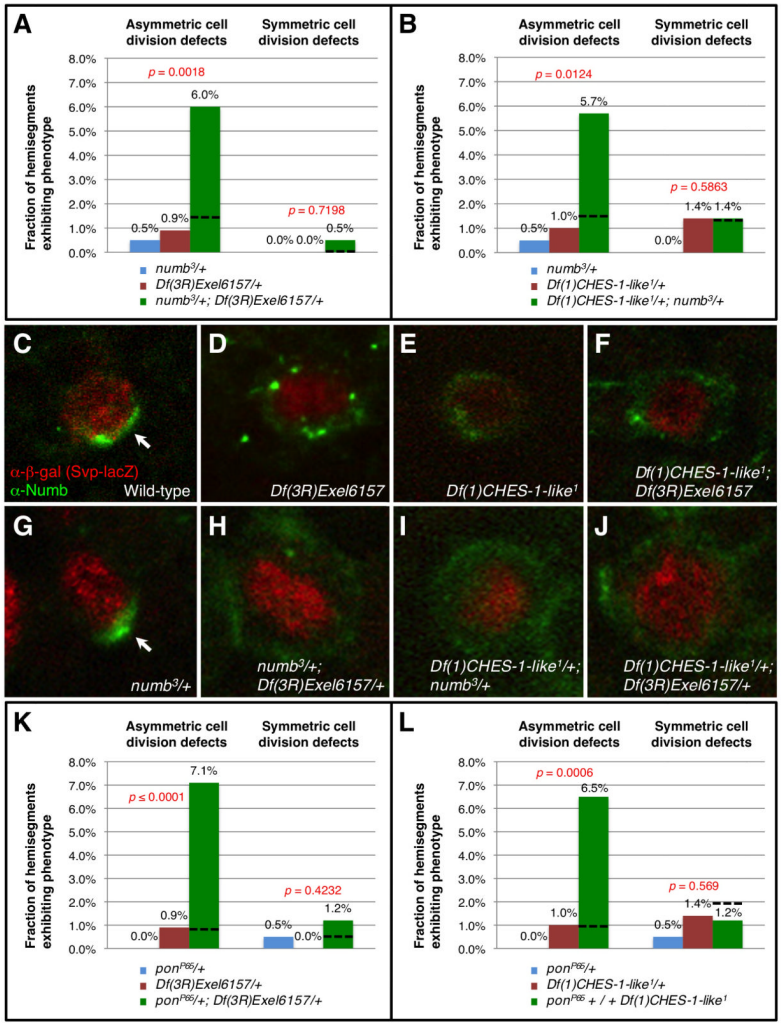

Figure 4. Asymmetric cell division defects in *jumu* and *CHES-1-like* mutants are a consequence of defective Numb protein localization in Svp cardiac cell progenitors

(A-B) Fraction of hemisegments exhibiting asymmetric and symmetric cell division defects for single and double heterozygotes of mutations in *jumu* and *numb* (A) and *CHES-1-like* and *numb* (B). The black dashed line indicates the expected results in the double heterozygotes if the phenotypes were purely additive.

(C) A dividing Svp-expressing cardiac progenitor cell from a wild-type embryo carrying the *svp-lacZ* enhancer trap, showing that Numb protein (green, arrow) is localized to a crescent at one pole of the β-galactosidase-expressing nucleus (red).

(D-J) Dividing Svp progenitor cells from embryos homozygous for the *jumu* null deficiency (D) or the *CHES-1-like* null mutation (E), the *CHES-1-like*; *jumu* double homozygote (F), an embryo heterozygous for the *numb* null mutation (G), and double heterozygotes for the *numb* null mutation and the *jumu* null deficiency (H), for the *CHES-1-like* and *numb* null mutations (I) and for the *CHES-1-like* null mutation and the *jumu* null deficiency (F), showing that in all but (G), Numb (green) fails to localize as in wild-type and instead is present as a diffuse halo surrounding the nuclei (red).

(K-L) Fraction of hemisegments exhibiting asymmetric and symmetric cell division defects for single and double heterozygotes of mutations in *jumu* and *pon* (K) and *CHES-1-like* and *pon* (L). The black dashed line indicates the expected results in the double heterozygotes if the phenotypes were purely additive.

See Also Table S2.

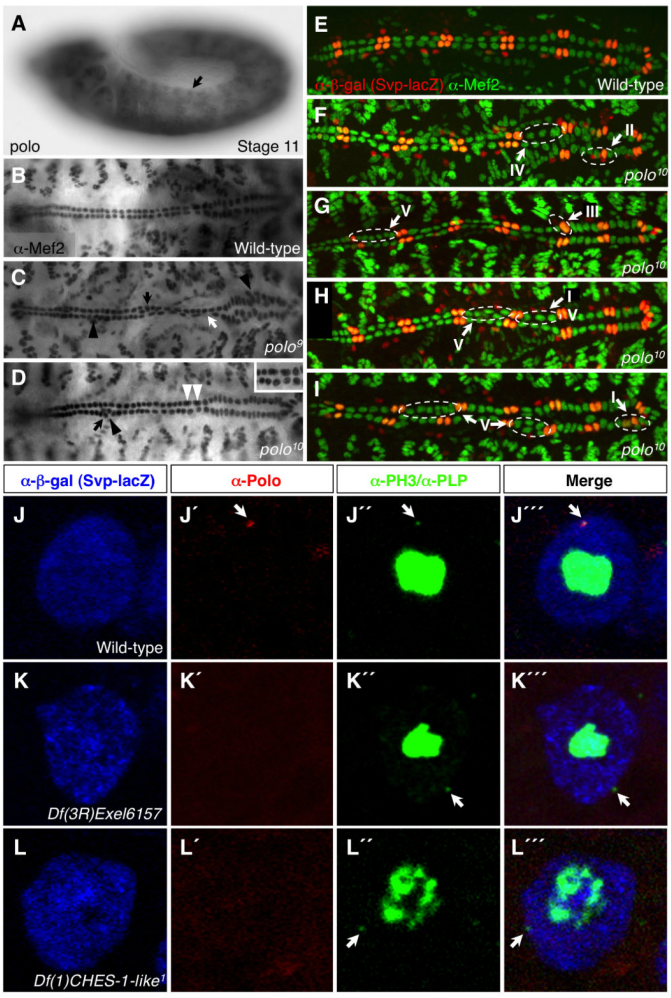

Figure 5. *polo* embryonic expression and loss-of-function cardiac phenotypes

(A) *polo* is expressed in the cardiac mesoderm (arrow) at stage 11.

(B-D) Embryos homozygous for strong hypomorphic mutations in *polo* (C-D) exhibit localized increases in CC number (black arrows), localized reductions in CC number (white arrows), incorrectly positioned CCs (black arrowheads), and enlarged CC nuclei (white arrowheads, inset), as compared to wild-type (B).

(E-I) Cardiac phenotypes in *polo* mutants are caused by the same cell division defects responsible for *jumu* and *CHES-1-like* mutant phenotypes (compare with Figure 3).

(J-J’’’) A representative dividing Svp-progenitor cell from a wild-type embryo that contains the *svp-lacZ* enhancer trap, showing the β-galactosidase-expressing nucleus (blue), Phospho-Histone H3 (a marker for mitotically dividing cells; diffuse green staining), Polo (red), and Pericentrin-like protein (PLP, a marker for the centrosome; small green dot indicated by the arrow).

(K-L’’’) Similarly stained examples of dividing Svp progenitor cells from *jumu* (K-K’’’) and *CHES-1-like* (L-L’’’) null mutants where Polo is not detected at the PLP-stained centrosomes (green, arrows).

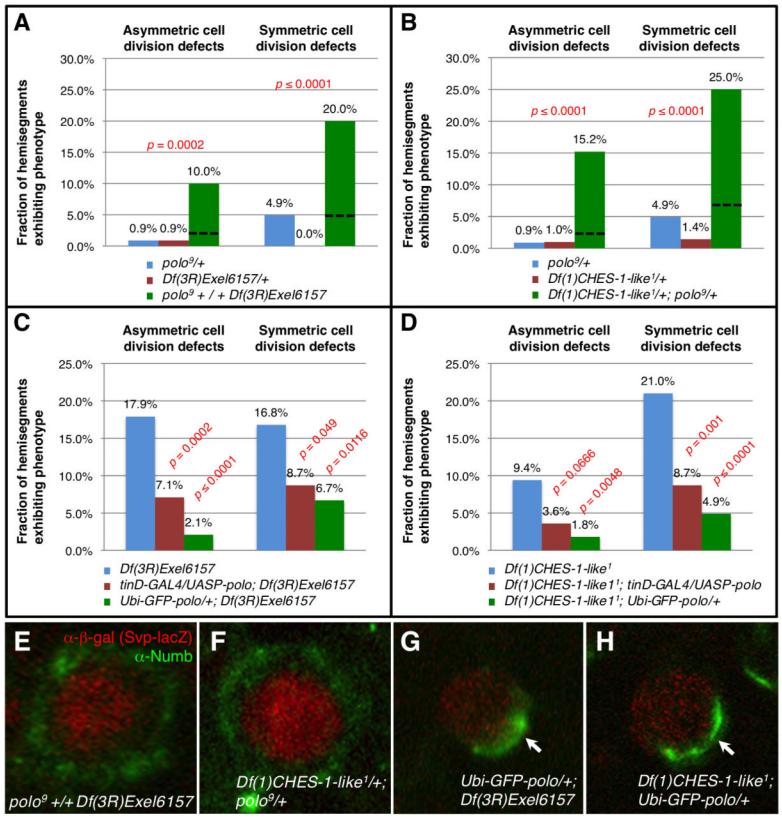

Figure 6. *polo* lies downstream of *jumu* and *CHES-1-like* in a pathway regulating the division of cardiac progenitor cells

(A-B) Fraction of hemisegments exhibiting asymmetric and symmetric cell division defects for single and double heterozygotes of mutations in *jumu* and *polo* (A) and *CHES-1-like* and *polo* (B). The black dashed line indicates the expected results in the double heterozygotes if the phenotypes were purely additive.

(C-D) Partial rescue of *jumu* (C) and *CHES-1-like* (D) homozygous mutant phenotypes by either ubiquitous *polo* expression or *polo* expression targeted to the cardiac mesoderm using *tinD-Gal4*.

See also Figure S4 and Tables S2 and S3.

(E-H) Dividing Svp progenitor cells showing that Numb protein localization is defective in double heterozygotes between mutations in *polo* and *jumu* (E) or *polo and CHES-1-like* (F), but is partially restored in *jumu* (G) or *CHES-1-like* (H) homozygotes ubiquitously expressing *polo*.

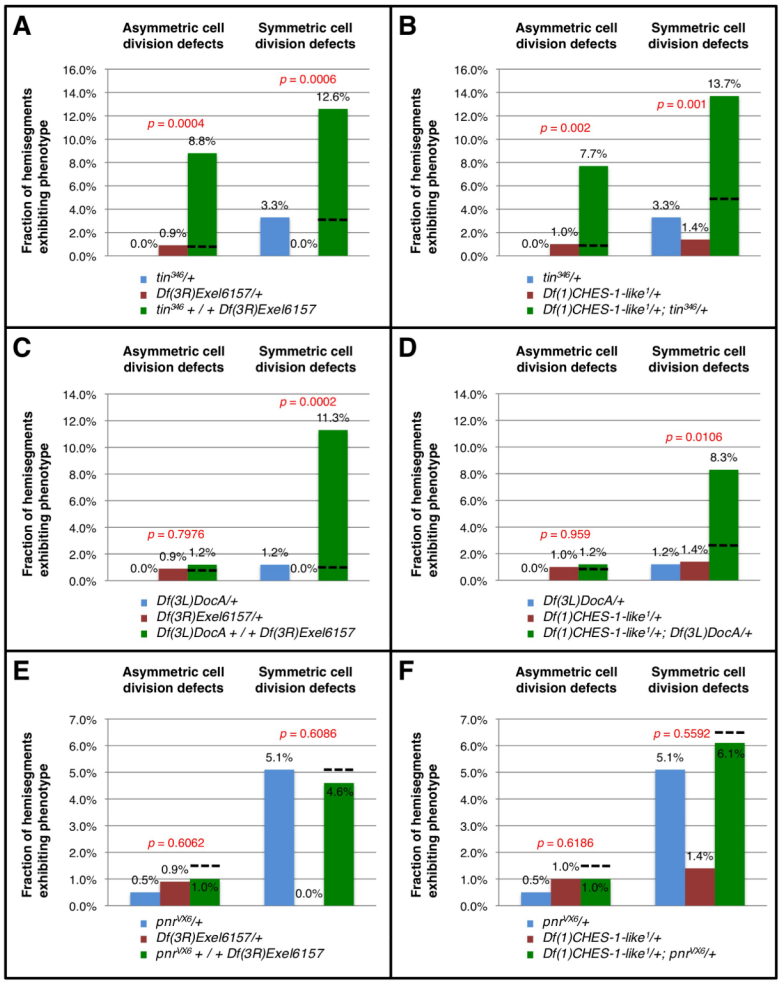

Figure 7. Synergistic interactions between the genes encoding the Jumu and CHES-1-like Fkh proteins and other known cardiogenic transcription factors

(A-B) Fraction of hemisegments exhibiting asymmetric and symmetric cell division defects for single and double heterozygotes of mutations in *jumu* and *tin* (A) and *CHES-1-like* and *tin* (B).

(C-D) Fraction of hemisegments exhibiting asymmetric and symmetric cell division defects for single and double heterozygotes of a deficiency, *Df(3L)DocA*, which excises all three *Doc* genes and a mutation in *jumu* (C), and *Df(3L)DocA* and a mutation in *CHES-1-like* (D).

(E-F) Fraction of hemisegments exhibiting asymmetric and symmetric cell division defects for single and double heterozygotes of mutations in *jumu* and *pnr* (E) and *CHES-1-like* and *pnr* (F).

In each case, the black dashed line indicates the expected results in the double heterozygotes if the phenotypes were purely additive. See also Table S2.